

MOL #67363

Regulation of M₃ Muscarinic Receptor Expression and Function by Transmembrane Protein 147

Erica Rosemond, Mario Rossi, Sara M. McMillin, Marco Scarselli, Julie G. Donaldson, and Jürgen Wess

Laboratory of Bioorganic Chemistry, National Institute of Diabetes and Digestive and Kidney Diseases (E.R., M.R., S.M.M., J.W.), and Laboratory of Cell Biology, National Heart, Lung, and Blood Institute (M.S., J.G.D.), Bethesda, Maryland

MOL #67363

Running title: M₃ muscarinic receptor interacts with Tmem147

Address correspondence to:

Jürgen Wess, PhD

Molecular Signaling Section

Lab. of Bioorganic Chemistry, NIH-NIDDK

Bldg. 8A, Room B1A-05

8 Center Drive MSC 0810

Bethesda, MD 20892-0810

Tel. 301-402-3589

Fax 301-480-3447

E-mail: jwess@helix.nih.gov

Manuscript length

Number of text pages: 40

Number of tables: 0

Number of figures: 11

Number of references: 40

Number of words in the Abstract: 248

Number of words in the Introduction: 736

Number of words in the Discussion: 912

ABBREVIATIONS: 3-AT, 3-amino-1,2,4-triazole; Cub, C-terminal portion of ubiquitin; FBS, Fetal bovine serum; GPCR, G protein-coupled receptor; HA tag, hemagglutinin tag; [³H]-NMS, N-[³H]-methylscopolamine; M3R, M₃ muscarinic receptor; MbYTH, membrane-based yeast two-hybrid; Nub, N-terminal portion of ubiquitin; PBS, phosphate-buffered saline; [³H]-QNB, [³H]-quinuclidinyl benzilate; SC medium, synthetic complete medium; Tmem147, transmembrane protein 147; TCA, trichloroacetic acid; YTH, yeast two-hybrid.

MOL #67363

ABSTRACT

The M₃ muscarinic acetylcholine receptor (M3R) regulates many fundamental physiological functions. To identify novel M3R-interacting proteins, we used a recently developed yeast two-hybrid screen (split ubiquitin method) to detect interactions among membrane proteins. This screen led to the identification of many novel M3R-associated proteins, including the putative membrane protein Tmem147. The amino acid sequence of Tmem147 is highly conserved among mammals but its physiological roles are unknown at present. We initially demonstrated that Tmem147 could be co-immunoprecipitated with M3Rs in co-transfected mammalian cells (COS-7 cells). Confocal imaging studies showed that Tmem147 was localized to ER membranes and that the Tmem147/M3R interaction occurred in the ER of co-transfected COS-7 cells, resulting in impaired trafficking of the M3R to the cell surface. To study the role of Tmem147 in modulating M3R function in a more physiologically relevant setting, we carried out studies with H508 human colon cancer cells which endogenously express M3Rs and Tmem147. Treatment of H508 cells with carbachol, a hydrolytically stable acetylcholine analog, promoted H508 cell proliferation and activation of the mitogenic kinase, p90RSK. Strikingly, siRNA-mediated knockdown of Tmem147 expression significantly augmented the stimulatory effects of carbachol on H508 cell proliferation and p90RSK activation. These effects were associated with an increase in the density of cell surface M3Rs. Our data clearly indicate that Tmem147 represents a potent negative regulator of M3R function, most likely by interacting with M3Rs in an intracellular compartment (ER). These findings may lead to new strategies aimed at modulating M3R activity for therapeutic purposes.

Introduction

The M₃ muscarinic acetylcholine receptor (M3R) is a prototypic member of the superfamily of class I GPCRs (Wess 1996). Following activation by muscarinic agonists, the M3R selectively activates G proteins of the G_q family (Wess 1996). Peripheral M3Rs play a key role in mediating the stimulatory actions of acetylcholine on smooth muscle and glandular tissues (Caulfield and Birdsall, 1998; Eglen, 2005; Wess et al., 2007). Interestingly, recent studies with M3R mutant mice suggest that the M3R represents a potential novel target for the treatment of several major pathophysiological conditions including type 2 diabetes (Gautam et al., 2006), colon cancer (Raufman et al., 2008), growth hormone deficiency (Gautam et al., 2009), and osteoporosis (Shi et al., 2010).

Unfortunately, muscarinic ligands that can activate or block the M3R with a high degree of selectivity are not available at present (Caulfield and Birdsall, 1998; Eglen, 2005; Wess et al., 2007). Moreover, since M3Rs are involved in many physiological functions, the potential use of M3R-selective ligands for therapeutic purposes is likely to be associated with significant side effects. We therefore initiated a new line of research in order to identify M3R-interacting proteins that modulate M3R expression and/or function. We speculated that this approach might eventually lead to new strategies aimed at modulating M3R function for therapeutic purposes.

Conventional yeast two-hybrid (YTH) screening approaches have been identified many GPCR-interacting proteins (Ritter and Hall, 2009; Bockaert et al., 2010). The use of traditional YTH technologies requires that the analyzed proteins are expressed in the nucleus. However, since full-length GPCRs usually require post-translational

MOL #67363

modifications, such as glycosylation or disulfide bond formation, for proper folding, the nucleus is an unfavorable environment for identifying GPCR-interacting proteins.

Furthermore, GPCRs and other transmembrane proteins tend to form aggregates in a non-membrane environment. To circumvent these difficulties, traditional YTH approaches usually employ soluble GPCR fragments, such as the cytosolic C-terminal domain or various intracellular loop regions. It is therefore likely that many GPCR-interacting proteins that require the presence of membrane-embedded full-length GPCRs for high affinity binding remained unidentified in conventional YTH screens.

In the present study, we used the split-ubiquitin membrane-based yeast two-hybrid (MbYTH) screen to identify novel M3R-interacting proteins (Stagljar and Fields, 2002; Iyer et al., 2005; Kittanakom et al., 2009). This system offers the great advantage that it does not require nuclear localization of the two interacting proteins in order to detect protein-protein interactions, as is the case with classic YTH approaches. This screening strategy depends on the association of the N- and C-terminal halves of ubiquitin (referred to as Nub and Cub, respectively), resulting in the release of an artificial transcription factor fused to the C-terminus of Cub by ubiquitin-specific proteases (Fig. 1). The transcription factor then enters the nucleus, causing the activation of specific reporter genes (*HIS3*, *ADE2*, and *LacZ*; Fig. 1). Specifically, we employed this system to screen a human brain cDNA library for proteins that can interact with the full-length rat M3R in yeast (strain name: NMY51; Dualsystems Biotechnology, Switzerland). For this work, we used a modified version of the M3R (M3R-Cub) that contained the C-terminal Cub sequence, followed by an artificial transcription factor, as the bait. The cDNA library was constructed in a fashion such that all encoded proteins contained the Nub sequence at

MOL #67363

their N-terminus. In this system, proteins that are able to interact with the M3R-Cub fusion protein will lead to the association of Nub and Cub, triggering the release of the artificial transcription factor from M3R-Cub.

An Ile->Gly point mutation in the Nub domain (NubI->NubG) greatly reduces the affinity of the Nub/Cub interaction such that the two protein fragments will no longer spontaneously interact (Iyer et al., 2005; Kittanakom et al., 2009). However, the interaction of the bait (attached to Cub) and the prey (attached to NubG) proteins allows the reconstitution of the two halves. The successful interaction between bait and prey proteins can be assayed by monitoring yeast growth in histidine-deficient media or by using a colorimetric test for the expression of β -galactosidase (Fig. 1).

Using this strategy, we identified many novel M3R-associated proteins, including Tmem147, an ER resident protein of unknown biological function. Biochemical and pharmacological studies demonstrated that Tmem147 acts as a potent negative regulator of M3R function, most likely by interfering with M3R trafficking to the cell surface. Our data suggest that Tmem147 and other M3R-associated proteins may represent novel targets for modulating M3R activity for the treatment of various human diseases including colon cancer.

Materials and Methods

Mammalian Expression Plasmids. Plasmids coding for the human M₁ and M₃ muscarinic receptors containing an N-terminal string of three hemagglutinin (HA) epitope tags (vector: pcDNA3.1(+)) were obtained from the Missouri S&T cDNA

MOL #67363

Resource Center (<http://www.cdna.org>). The mammalian expression plasmid coding for the human V₂ vasopressin receptor carrying an N-terminal HA tag has been described previously (Schöneberg et al., 1996). The human Tmem147 cDNA in the pOTB7 vector (NM_032635.2) was obtained from ATCC (Manassas, VA). This construct was originally generated by the I.M.A.G.E. Consortium/Mammalian Gene Collection. The Tmem147 coding sequence was subcloned into the pcDNA3.1(-) vector, and a FLAG epitope tag (DYKDDDDK) was inserted after the methionine start codon by using standard PCR mutagenesis techniques. The coding sequences of all constructs were verified by sequencing.

Yeast Expression Plasmids. The rat M3R coding sequence containing an N-terminal HA tag (Schöneberg et al., 1995) was subcloned into the pAMBV4 plasmid (Dualsystems Biotech, Schlieren, Switzerland). To generate the M3-Cub construct, overlapping PCR was used to fuse the last amino acid of the M3R coding sequence in frame with the Cub portion of the pAMBV4 plasmid.

Yeast Liquid Growth Bioassay. For radioligand binding and functional studies, the M3R-Cub coding sequence was subcloned into the p416GPD plasmid (Mumberg et al., 1995; Erlenbach et al., 2001) via standard subcloning techniques. A p416GPD-based plasmid coding for the full-length rat M3R (without the Cub portion) has been generated previously (Erlenbach et al., 2001). The two plasmids were transformed into the MPY578q5 yeast strain (Pausch et al., 1998; Erlenbach et al., 2001). This strain contains a genetically modified G protein α -subunit (Gpa1p) in which the last 5 amino acids of

MOL #67363

Gpa1p (KIGII) are replaced with the homologous mammalian G α q (EYNLV) sequence, resulting in agonist-stimulated M3R/G protein coupling and yeast growth in selective media. Overnight yeast cultures were diluted to 1×10^5 cells/ml in synthetic complete medium (SC medium) lacking histidine and uracil and containing 5 mM of 3-amino-1,2,4-triazole (3-AT). Yeast growth was monitored by recording increases in absorbance at 630 nm in the presence of increasing concentrations of carbachol. Concentration-response curves were analyzed using GraphPad Prism 4.0 (GraphPad Software, San Diego, CA).

Isolation of Yeast Crude Membranes and Radioligand Binding Assays. Crude yeast membrane preparations were prepared from fresh 2 l yeast cultures, using a previously described glass bead method (Erlenbach et al., 2001). N-[3 H]-Methylscopolamine ([3 H]-NMS, 79-83 Ci/mmol; Perkin-Elmer, Boston, MA) saturation binding assays were carried out using yeast membrane homogenates (250 μ g protein/tube) as described (Erlenbach et al., 2001). Briefly, the binding buffer consisted of 25 mM phosphate buffer (pH 7.4) containing 5 mM MgCl₂. Binding reactions were carried out for 3 h at 25 °C in a 1 ml volume. Six different concentrations of [3 H]NMS were used. Nonspecific binding was determined in the presence of 10 μ M atropine. Radioligand binding data were analyzed using GraphPad Prism 4.0 (GraphPad Software).

Culture and Transient Transfection of COS-7 Cells. COS-7 cells were maintained in Dulbecco's modified Eagle's medium supplemented with 10% fetal bovine serum (FBS), 2 mM L-glutamine, 100 units/ml penicillin, and 100 μ g/ml streptomycin at 37 °C in a

MOL #67363

humidified 5% CO₂ incubator. About 24 h prior to transfection, $\sim 1 \times 10^6$ cells were seeded into 100 mm dishes. Cells were transfected with 4 μ g of plasmid DNA per dish. In co-transfection experiments, 2 μ g of each plasmid were used. Transfections were carried out using Lipofectamine and Plus reagent as per the manufacturer's instructions (Invitrogen, Carlsbad, CA). Cells were collected 48 h after transfection.

Calcium Assay (COS-7 Cells). We employed FLIPR technology (Molecular Devices, Sunnyvale, CA) to measure carbachol-mediated increases in intracellular calcium levels using transiently transfected COS-7 cells. Assays were carried out in duplicate in 96-well plates, as described in detail previously (Scarselli et al., 2007). E_{\max} and EC_{50} values were obtained from carbachol concentration-response curves analyzed by using GraphPad Prism 4.0 software (GraphPad Software).

Confocal Microscopy and Antibodies (COS-7 Cells). COS-7 cells were transiently transfected with plasmid DNA, as described above. About 24 h after transfection, cells were fixed with 2% paraformaldehyde for 10 min and then washed with phosphate-buffered saline (PBS) containing 10% FBS. All studies were carried out with cells that had been permeabilized with 0.2% saponin. To facilitate the detection of the M3R protein, we used a plasmid coding for a modified version of the human M3R containing three N-terminal HA epitope tags (M3R-HA). To visualize the expression of Tmem147, we generated a human Tmem147 construct with an N-terminal FLAG tag (Tmem147-FLAG). Expression of the M3R-HA protein was detected with a mouse anti-HA monoclonal antibody (16b12, IgG1; Covance, Princeton, NJ). The Tmem147-FLAG

MOL #67363

protein was visualized using a rabbit polyclonal anti-FLAG antibody (Sigma, St. Louis, MO). After extensive washing, Alexa-conjugated fluorescent secondary antibodies (goat anti-mouse [Alexa-488] or goat anti-rabbit [Alexa-594]) were used (Invitrogen, Carlsbad, CA). To determine the intracellular localization of Tmem147, different marker proteins were employed. The mouse monoclonal GM130 and EEA1 antibodies (BD Biosciences, Franklin Lakes, NJ) were used to stain the Golgi complex and early endosomes, respectively. The pDsRed2-ER plasmid (a kind gift from Dr. David Sibley, NIH) served to visualize the ER (Free et al., 2007). All images were obtained using a 510 LSM confocal microscope (Zeiss, Germany) with a 63x 1.3 numerical aperture PlanApo objective (for experimental details, see Scarselli and Donaldson, 2008).

Co-immunoprecipitation Studies (COS-7 Cells). COS-7 cells that had been co-transfected with the M3R-HA and Tmem147-FLAG constructs were collected 48 h after transfection by scraping with ice-cold PBS and centrifugation for 10 min at 4 °C at 1000 x g. Cells from one 100 mm plate were resuspended in 1 ml of solubilization buffer (50 mM HEPES, 1 mM EDTA, 10% glycerol, 1% Triton X-100, 150 mM NaCl, 50 mM NaF, 40 mM sodium pyrophosphate, and Roche complete protease inhibitor cocktail, pH 7.4) for 2 h on a rock-and-roll shaker at 4 °C. Subsequently, insoluble material was separated by centrifugation at 20,000 x g for 30 min at 4 °C. Samples were then pre-cleared with 20 µl of protein-A agarose (Santa Cruz Biotechnology, Santa Cruz, CA) for 1 h on a rock-and-roll shaker at 4 °C and separated by centrifugation at 20,000 x g for 5 min at 4 °C. In the next step, 20 µl of agarose-conjugated mouse anti-HA monoclonal antibody (clone HA-7; Sigma) or 2 µl of rabbit anti-FLAG polyclonal antibody (Sigma, St. Louis, MO)

MOL #67363

was added to the sample and incubated overnight on a rock-and-roll shaker at 4 °C. On the next day, 20 µl of protein-A agarose was added to the samples treated with the anti-FLAG antibody, followed by a 1 h incubation on a rock-and-roll shaker at 4 °C. To collect immunoprecipitated products, samples were centrifuged at maximum speed in an Eppendorf 5417R tabletop centrifuge at 4 °C and washed three times with 1 ml of solubilization buffer containing 200 mM NaCl and once with TE (pH 7.4). Subsequently, 45 µl of 2x NuPage LDS sample buffer was added to the agarose beads, followed by a 30 min incubation at 50 °C. Samples were then quickly vortexed and centrifuged at maximum speed for 5 min, and DTT was added to a final concentration of 10 mM. Samples were run on NuPage 4-12% Bis-Tris gels with MOPS SDS running buffer (Invitrogen, Carlsbad, CA). Proteins were transferred onto nitrocellulose membranes using NuPage transfer buffer (Invitrogen). Membranes were blocked with 5% milk and first probed with either goat anti-M3R polyclonal antibody (C-20; Santa Cruz Biotechnology) or rabbit polyclonal anti-FLAG antibody (Sigma, St. Louis, MO), followed by incubation with donkey anti-goat IgG-HRP (1:10,000; Santa Cruz Biotechnology) or donkey anti-rabbit IgG-HRP (1:10,000; Amersham/GE Healthcare, Piscataway, NJ) secondary antibody, respectively. Immunoreactive bands were detected using Pierce SuperSignal West Pico Chemiluminescent Substrate and Pierce CL-XPosure Film (Pierce, Rockford, IL).

Culture and siRNA Treatment of H508 Cells. H508 human colon cancer cells (source: ATCC) were grown in T175 flasks (Costar, Cambridge, MA) in RPMI-1640 medium (Invitrogen) containing 10% FBS at 37 °C in a humidified 5% CO₂ incubator. siRNA was

MOL #67363

introduced into H508 cells via nucleofection when the cells were about 75-80% confluent. The following siRNAs were used (source: Ambion, Austin, TX): scrambled negative control siRNA (# 4390843), Tmem147 siRNA (ID: s20403), or human M3R siRNA (ID: s60845). Cell pellets were re-suspended according to the manufacturer's instructions (Amaxa Biosystems, Gaithersburg, MD), and $\sim 1-2 \times 10^6$ cells were placed into tubes containing 5 μ l of Tmem147 siRNA or control siRNA (20 μ M each). The cells were then placed into the nucleofection vials and electroporated using program A-23 of the Nucleofector II device and the Cell Line Nucleofector Kit V as per the manufacturer's instructions (Amaxa Biosystems). Electroporated cells were immediately placed into 12-well plates (Costar) for binding or 6-well plates (Costar) for Western blotting experiments, respectively. For cell proliferation assays, electroporated cells were seeded into 96-well plates (Costar). About 24 h after electroporation, H508 cells were washed with PBS, and the medium was replaced with RPMI-1640 medium containing 100 μ M of carbachol. After three days of culture, cells received fresh medium (RPMI-1640 containing 100 μ M of carbachol) and were cultured for two more days. Experiments were carried out 3-5 days after nucleofection.

Real-time qRT-PCR Studies (H508 Cells). Three to five days after nucleofection with siRNAs, total RNA was extracted from H508 cells using the Qiagen RNeasy kit as per manufacturer's instructions (Qiagen, Germantown, MD). RNA (~ 1 μ g) was reverse transcribed using Superscript III First-strand Synthesis SuperMix for qRT-PCR as per the manufacturer's instructions (Invitrogen). qPCR was accomplished on a 7900 HT Fast Real-Time PCR machine (Applied Biosystems, Foster City, CA) using SYBR Green

MOL #67363

PCR Master Mix (Applied Biosystems). The following primers were used: Tmem147 (human), F-5'-tacaacgccttctggaatgc, R-5'-ccaatgaagtcataatgc; M3R (human), F-5'-atcgggtctggcttgggtc, R-5'-cccggaggcacagttctc; GAPDH (internal control), F-5'-ccccatgggtgtctgagcg, R-5'-cgacagtcagccgcattt. qPCR experiments were carried out as described in detail by Cheng et al., 2007).

To monitor human M₁-M₅ muscarinic receptor transcript levels in H508 cells, we also carried qRT-PCR studies with RNA prepared from H508 cells that had not been treated with siRNA. For these studies, we used the following primer pairs: M₁, F-5'-gggcagtgtctacatccagtcc, R-5'-cgtgctcggttctctgtctccc; M₂, F-5'-catatcccagccagcaagagc, R-5'-gaggcaacagcactgactgagg; M₃, F-5'-cgagacgagagccatctactcc, R-5'-gaccagggacatcctttccgc; M₄, F-5'-actgtcgtgggcaacatcctgg, R-5'-cttggtgacgcagaagtagcgg; M₅, F-5'-acctgctcagcttagcctgtgc, R-5'-tggaactgtccgcttcccaacc (Genbank accession numbers: M₁, AF498915; M₂, AF498916; M₃, AF498917; M₄, AF498918; M₅, AF498919).

H508 Cell Proliferation Assay. The proliferation of H508 cells was determined using the sulforhodamine B (SRB) colorimetric assay, as described in detail previously (Skehan et al., 1990; Cheng et al., 2007). After nucleofection, H508 cells were seeded into 96-well plates (~20,000 cells per well; Corning Inc., Corning, NY) and then allowed to recover for 24 h in RPMI-1640 medium containing 10 % FBS. The medium was then replaced with serum-free RPMI-1640 medium. Cells were allowed to grow for five more days at 37 °C in a 5% CO₂/95% air atmosphere, either in the absence or presence of 100 μM carbachol. After this five day growth period, cells were fixed by adding 50%

MOL #67363

trichloroacetic acid (TCA) to the growth medium (final concentration of TCA: 10%), incubated for 1 h at 4 °C, and then washed five times with distilled water to remove the TCA. Cells were stained for 30 min at room temperature with 50 µl of 0.4% (w/v) SRB dissolved in 1% acetic acid and then rinsed four times with 200 µl of 1% acetic acid. Protein-bound dye was extracted with 100 µl of 10 mM Tris for 5-10 min on a plate shaker. Color development (OD) was measured between 540-590 nm on a BioTek ELx808 spectrophotometer (BioTek Instruments, Winooski, VT).

Determination of Cell Surface and Total Cellular Muscarinic Receptor Levels (H508

Cells). H508 cells were cultured as described in the previous paragraph. Five days after siRNA treatment, intact H508 cells grown in 12-well plates in the presence of carbachol (100 µM) were incubated with a saturating concentration (1 nM) of [³H]NMS), a hydrophilic muscarinic radioligand that only labels cell surface muscarinic receptors. To determine the levels of total cellular muscarinic receptors, we carried out analogous studies using a saturating concentration (1 nM) of [³H]-quinuclidinyl benzilate ([³H]-QNB; 50.5 Ci/mmol; Perkin-Elmer, Boston, MA), a membrane-permeable muscarinic radioligand. After two washes with binding buffer (25 mM phosphate buffer containing 5 mM MgCl₂, pH 7.4), cells were incubated in 0.5 ml of binding buffer with 1 nM of [³H]NMS for 90 min at 37 °C. Non-specific binding was measured in the presence of 1 µM atropine. Following the 90 min incubation period, cells were washed three times with ice-cold PBS and scraped off the plates using 500 µl PBS containing 1% Triton X. Ten ml of Hydrofluor scintillation cocktail (National Diagnostics, Manville, NJ) was then added to the samples, and radioactivity was counted on a Wallac WinSpectral 1414 liquid

MOL #67363

scintillation counter (Perkin Elmer, Boston, MA). Protein concentrations were determined by using a Bradford assay kit (Pierce, Rockford, IL).

Western Blotting Studies (H508 Cells). Five days after siRNA treatment, intact H508 cells grown in 6-well plates in the presence of carbachol (100 μ M) were first washed and then incubated with 1 ml of RPMI-1640 medium at room temperature in presence or absence of 500 μ M of carbachol for 10 min. Cells were then scraped off the plates using 250 μ l of Western blotting buffer (150 mM NaCl, 10 mM Tris HCl, 1% deoxycholate, 1% NP-40, 0.1% SDS, and 4 mM EDTA) in the presence of protease inhibitors (Complete Midi; Roche Diagnostics Inc., Indianapolis, IN). Proteins were separated on 10% Tris-glycine gels (Sigma) using an SDS-based loading buffer (Quality Biological Inc., Gaithersburg, MD) and then blotted onto nitrocellulose membranes (0.45 μ m pore size, Sigma). The phosphorylated (active) form of p90RSK (phospho-p90RSK) was detected via Western blotting using the phospho-p90RSK antibody from Cell Signaling (Irvine, CA) as the primary antibody (1:1,000 dilution). Binding of the primary antibody was detected using an HRP-linked secondary anti-rabbit IgG antibody (1:4,000 dilution; Cell Signaling). For control purposes, all blots were reprobed with a β -actin antibody (1:1,000 dilution; Cell Signaling). Bands were detected by the GeneGnome capture and analysis system (Syngene, Frederick, MD). Band intensities were quantified using the ImageJ program (NIH, Bethesda, MD), and data were analyzed using GraphPad Prism 4.0 (GraphPad Software).

MOL #67363

RT-PCR Analysis of M3R and Tmem147 Expression in Different Mouse Tissues.

cDNAs were prepared from different mouse tissues derived from C57BL/6NTac mice as described by Li et al. (2009). To detect M3R and Tmem147 transcripts, cDNAs were amplified via PCR using the following gene-specific primers pairs: M3R-F, 5'-ACCTGTTACACGACCTACATCA; M3R-R, 5'-AGTGAGTGGCCTGGTAATAGAAA; Tmem147-F, 5'-CCACACCTTCCGGCCTGCTG; Tmem147-R, 5'-GCCAAGGTGCTGAGGGCCAG. The PCR amplicon sizes were 158 bp (M3R) and 156 bp (Tmem147), respectively. The PCR cycling conditions were as follows: 95 °C for 2 min followed by 33 cycles at 95 °C for 30 s, 56 °C for 60 s, and 72 °C for 60 s. PCRs were carried out in a final volume of 30 µl containing 3 µl of the RT reaction product (corresponding to ~0.1 mg RNA), 3 µl of GeneAmp 10 x PCR buffer (Applied Biosystems), 1 mM of each dNTP, 1.3 µM of each PCR primer, and 1 unit of recombinant AmpliTaq Gold (Applied Biosystems).

Results

MbYTH Bait Selection And Characterization. In this study, we employed the membrane-based, split-ubiquitin yeast two-hybrid system (MbYTH) to identify novel M3R-interacting proteins. We first cloned the rat M3R coding sequence into the pAMBV4 bait vector (Dualsystems Biotechnology, Switzerland). The resulting yeast expression plasmid codes for a modified version of the M3R receptor in which the C-terminus of the receptor is fused to the C-terminal portion of ubiquitin (Cub) followed by an artificial transcription factor (Fig. 1). For the sake of simplicity, we refer to this 'bait

MOL #67363

receptor' as M3-Cub in the following. The pAMBV4-M3-Cub plasmid was then transformed into the NMY51 yeast strain (Dualsystems Biotechnology). [³H]NMS saturation binding studies carried out with yeast membranes demonstrated that the M3-Cub protein was able to bind [³H]NMS with high affinity ($pK_D = 9.50 \pm 0.49$; $B_{max} = 7.4 \pm 2.4$ fmoles/mg; $n = 3$).

To confirm that the M3-Cub receptor was functional in yeast, we next cloned the M3-Cub coding sequence into the p416GPD yeast expression vector (Mumberg et al., 1995; Erlenbach et al., 2001). The resulting plasmid (p416GPD-M3-Cub) was then transformed into the MPY578q5 yeast strain (Pausch et al., 1998; Erlenbach et al., 2001). For comparison, a p416GPD-based plasmid coding for the wild-type (WT) rat M3R (WT-M3) was also transformed into the same yeast strain. Due to several genetic modifications, the MPY578q5 yeast strain requires productive M3R/G protein coupling for growth in histidine-deficient media (see Materials and Methods for details; Erlenbach et al., 2001). Importantly, the MPY578q5 strain harbors a mutant version of the *GPA1* gene coding for a hybrid yeast/mammalian G protein α subunit in which the last five amino acids of Gpa1p were replaced with the corresponding mammalian $G\alpha_q$ residues (Erlenbach et al., 2001). To monitor muscarinic agonist (carbachol)-induced M3R activation, we measured yeast growth in histidine-deficient media ('yeast liquid growth bioassay'; Fig. 2). Carbachol treatment resulted in concentration-dependent growth of both the M3-Cub- and WT-M3-expressing yeast strains (Fig. 2). No growth response was observed with a control yeast strain transformed with vector DNA (p416GPD; Fig. 2). Carbachol stimulated the growth of M3-Cub- and WT-M3-expressing yeast strains with similar potency (carbachol EC_{50} values: M3-Cub, 4.5 ± 0.8 μ M; WT-M3, 4.9 ± 2.4 μ M;

MOL #67363

n=3), indicating that the C-terminal Cub tag did not interfere with M3R function in yeast. Taken together, the results of the radioligand binding and functional assays clearly indicate that the M3-Cub receptor is functional in yeast, indicative of proper receptor folding.

Optimization of Screening Conditions. We carried out a series of pilot experiments to optimize the conditions for the planned MbYTH screen (in order to reduce the number of false positives). The pAMBV4-M3-Cub plasmid coding for the M3-Cub bait was transformed into the NMY51 yeast strain, together with control plasmids coding for Alg5-NubI (positive control) or Alg5-NubG (negative control), or pADL-Nx (empty vector). Alg5-NubI is a yeast membrane protein modified with a WT Nub tag. The NubI tag usually interacts spontaneously with any Cub-containing construct (Iyer et al., 2005; Kittanakom et al., 2009). The Nub portion of Alg5-NubG contains the Ile->Gly point mutation at position 13, reducing the affinity of the Nub tag for Cub (Iyer et al., 2005; Kittanakom et al., 2009). This mutant Nub tag will only interact with a Cub-containing bait when the two tags are brought into proximity through an interaction between the attached bait and prey proteins (Iyer et al., 2005; Kittanakom et al., 2009).

We initially plated the co-transformants on -Leu/-Trp plates to select for yeast clones containing both the Cub- and Nub-containing plasmids. We then monitored the growth of co-transformants in -Leu/-Trp/-His/-Ade media (the proper association of Nub and Cub fragments results in the activation of the *HIS3* reporter gene and allows yeast growth in media lacking histidine; for details, see Materials and Methods). To suppress

MOL #67363

background growth, 3-AT (10 or 25 mM), an agent that blocks one of the key enzymes involved in histidine biosynthesis, was added to the medium.

As expected, co-transformation of the M3-Cub construct with pADL-Nx vector DNA did not result in yeast growth in histidine-deficient media (Fig. 3). However, co-transformation of M3-Cub with Alg5-NubI allowed yeast growth under the same experimental conditions (independent of the absence or presence of AT), indicating that the Cub portion of the M3-Cub fusion protein was folded properly. In contrast, M3-Cub was unable to interact with Alg5-NubG under high stringency conditions (10 or 25 mM AT; Fig. 3). To minimize background growth (false negatives), we therefore decided to carry out the planned MbYTH screen in the presence of 25 mM AT.

Identification of Candidate Proteins Able to Interact with M3-Cub in Yeast. Since the M3R is widely expressed throughout the brain, we used the M3-Cub construct as a bait to screen the NX031 human adult brain cDNA library for M3R-interacting proteins (complexity of the library: $\sim 2 \times 10^6$ independent clones; Dualsystems Biotechnology). This cDNA library was constructed in a fashion that all encoded proteins contained an N-terminal NubG tag. We transformed the NX031 library with the M3-Cub construct and then screened 2.4×10^6 transformants for growth on selective media (-Leu/-Trp/-His/-Ade) containing 25 mM 3-AT. This screen led to the identification of 68 potential M3R-interacting proteins, including proteins known to associate with the M3R such as calmodulin 2 (Lucas et al., 2006) or ARF1 (Mitchell et al., 2003). The identity of the Nub-containing proteins was verified by DNA sequencing, followed by BLAST analysis.

MOL #67363

The recovered proteins were classified into eight categories (for details, see Supplemental Table 1).

In a series of control experiments, we co-transformed all recovered Nub clones into the NMY51 yeast strain with either M3-Cub or Alg5-Cub. The co-transformants were then assayed for growth in selective media and their ability to induce color formation in a β -galactosidase assay. This analysis confirmed that all recovered Nub clones were able to interact with the M3-Cub protein in yeast. However, none of the Nub proteins was capable of interacting with Alg5-Cub, indicative of the selectivity of the interaction of M3-Cub with the recovered Nub proteins.

Interestingly, one full-length protein, transmembrane protein 147 (Tmem147; alternative name: NIFIE14; NM_032635.2), was recovered 11 independent times. Tmem147 is predicted to represent an integral membrane protein that spans the membrane six or seven times (HHMTOP or TMHMM programs). It consists of 224 amino acids and has a calculated molecular mass of 26.2 kDa. The amino acid sequence of Tmem147 is highly conserved among mammalian species (the human, rat, bovine and mouse sequences are 99% identical; see Supplemental Fig. 1 for details). The UniGene database for EST profiles indicates that Tmem147 is widely expressed throughout the body. The function of Tmem147 remains unknown at present. We therefore decided to carry out studies with mammalian cells to examine the potential effect of Tmem147 on regulating M3R expression and function.

Tmem147 Interacts With the M3R in Co-transfected Mammalian Cells. We first wanted to verify that the M3R/Tmem147 interaction also occurred in mammalian cells.

MOL #67363

Since it was difficult to detect M3R/Tmem147 complexes in physiological tissues because of the lack of suitable antibodies, we carried out co-immunoprecipitation studies using co-transfected COS-7 cells. To facilitate these experiments, we generated a human Tmem147 construct with an N-terminal FLAG tag (Tmem147-FLAG) and used a modified version of the human M3R containing three N-terminal HA epitope tags (M3R-HA).

We first prepared membranes from COS-7 cells co-transfected with the Tmem147-FLAG and M3R-HA constructs. Following membrane lysis, the M3R-HA was immunoprecipitated with an anti-HA antibody, followed by Western blotting studies using an anti-FLAG antibody (Fig. 4, left panel). The anti-FLAG antibody detected a single immunoreactive band, corresponding in size to Tmem147-FLAG (~30 kDa). In a reciprocal fashion, Tmem147-FLAG was immunoprecipitated with an anti-FLAG antibody, followed by Western blotting studies using an anti-HA antibody to identify Tmem147-associated M3Rs (Fig. 4, right panel). The anti-HA antibody detected a broad spectrum of immunoreactive species ranging in size from ~70 to >250 kDa. The estimated molecular mass of the M3R-HA protein is ~70 kDa. However, the M3R is known to undergo heterogeneous glycosylation at five N-terminal Asn residues (Wess, 1996) and, like most other GPCRs, can form dimeric or oligomeric complexes (Zeng and Wess, 1999; Goin and Nathanson, 2006). These factors are most likely responsible for the rather broad spectrum of M3R bands detected by the anti-HA antibody. The Tmem147-FLAG and M3R-HA bands were not observed in mock co-immunoprecipitation experiments in which cell lysates were incubated with protein-A agarose only (in the absence of antibodies) or in control experiments in which membranes prepared from

MOL #67363

COS-7 cells expressing either Tmem147-FLAG or M3R-HA had been mixed (Fig. 4).

The results of the co-immunoprecipitation studies strongly support the concept that Tmem147 interacts with the M3R in mammalian cells.

To examine whether Tmem147 can also bind to other muscarinic receptor subtypes or other class I GPCRs, we carried out analogous co-immunoprecipitation studies with COS-7 cells co-transfected with Tmem147-FLAG and HA-tagged versions of the M₁ muscarinic or the V₂ vasopressin receptor subtypes. These studies demonstrated that Tmem147-FLAG could be co-immunoprecipitated with either of the two receptors (Supplemental Fig. 2), suggesting that Tmem147 is able to interact not only with the M3R but also with other class I GPCRs.

Tmem147 is Found in the ER of Transfected COS-7 Cells. Since it was difficult to detect the expression of endogenous Tmem147 protein in cell lines or physiological tissues because of the lack of suitable antibodies, we studied the subcellular distribution of Tmem147-FLAG after transient expression in COS-7 cells. Confocal microscopic images showed that Tmem147 was not found on the cell surface but was localized to ER membranes (Fig. 5A). Tmem147 was not present in the Golgi complex (Fig. 5B) or in early endosomes (Fig. 5C), as shown with organelle-specific marker proteins.

Tmem147 Causes Retention of the M3R in the ER of Co-transfected COS-7 Cells.

To examine the effect of Tmem147 on the subcellular distribution of the M3R, we carried out studies with COS-7 cells co-transfected with the M3R-HA and Tmem147-FLAG constructs. When expressed alone, the M3R-HA receptor was expressed predominantly

MOL #67363

on the cell surface, as studied via confocal microscopic analysis of permeabilized cells stained with an anti-HA antibody (Fig. 6A). In contrast, the Tmem147-FLAG protein could only be detected intracellularly, as observed by treating cells with an anti-FLAG antibody (Fig. 6C; also see Fig. 5). Strikingly, following co-expression of the two constructs (M3R-HA and Tmem147-FLAG), cell surface expression of the M3R-HA receptor was barely detectable, and the receptor protein was co-localized with Tmem147-FLAG in the ER (Fig. 6D-F).

Tmem147 Expression Impairs M3R Function in Co-transfected COS-7 Cells. To examine the effect of Tmem147 expression on M3R function, we carried out additional studies using COS-7 cells co-transfected with M3R-HA and Tmem147 plasmid DNA (or vector DNA as a control). Consistent with the outcome of the M3R localization experiments, [³H]NMS saturation binding studies showed a pronounced reduction (by ~75%) in M3R density following co-expression with Tmem147 (Fig. 7A). [³H]NMS binding affinities (pK_D values) for the M3R were not significantly affected by co-expression with Tmem147: M3R + vector (control), 9.60 ± 0.22; M3R + Tmem147, 9.98 ± 0.26 (n=3).

To assess the functional consequences of Tmem147 co-expression on M3R function, we measured carbachol-mediated increases in intracellular calcium levels in co-transfected COS-7 using FLIPR technology. Carbachol treatment resulted in concentration-dependent calcium responses in both control cells (co-transfected with M3R and vector DNA) and in cells co-expressing M3R and Tmem147 (Fig. 7B).

MOL #67363

However, M3R-mediated maximum responses (E_{\max} values) were reduced by ~20% in the presence of Tmem147 ($p < 0.05$; Fig. 7B).

Studies With H508 Human Colon Cancer Cells Endogenously Expressing M3Rs and Tmem147. To study the effects of Tmem147 on M3R function in a more physiological setting, we used H508 human colon cancer cells as a model system. Frucht et al. (1999) previously demonstrated that H508 cells express significant numbers of endogenous M3Rs. Real-time qRT-PCR studies indicated that H508 cells almost exclusively express the M3R subtype (the four remaining muscarinic receptor subtypes are expressed only at very low levels; Fig. 8A).

Several studies have shown that muscarinic agonists stimulate the proliferation of H508 cells, most likely by activation of the ERK pathway and/or transactivation of epidermal growth factor receptors (Frucht et al., 1999; Cheng et al., 2003; Cheng and Raufman; 2005; Xie et al., 2009). To study the potential effect of Tmem147 on M3R-mediated stimulation of H508 cell proliferation, we treated H508 cells with either control siRNA (scrambled siRNA; cat. # 4390843, Ambion) or Tmem147 siRNA (ID s20403, Ambion). Subsequently, we incubated H508 cells for 5 days in the absence or presence of carbachol (100 μ M), and then determined cell growth by employing a colorimetric assay (Frucht et al., 1999; Cheng et al., 2003; Cheng and Raufman; 2005; Xie et al., 2009). Under these experimental conditions, carbachol (100 μ M) exerts a near-maximal effect on H508 cell proliferation (Frucht et al., 1999). Real-time qRT-PCR studies showed that treatment of H508 cells with Tmem147 siRNA virtually abolished Tmem147 mRNA expression (Fig. 8B). On the other hand, M3R mRNA levels remained unaffected

MOL #67363

following siRNA-mediated silencing of Tmem147 expression (Fig. 8B). As expected, carbachol treatment promoted the proliferation of H508 cells electroporated with control siRNA (~15% increase in growth compared to cells not treated with carbachol; Fig. 9). Interestingly, this response was significantly more pronounced ($p < 0.05$) in H508 cells electroporated with Tmem147 siRNA (~22% increase in growth compared to cells not treated with carbachol; Fig. 9). Carbachol-promoted H508 cell growth could be completely prevented by incubation of cells with atropine (1 μ M; Fig. 9).

Stimulation of H508 cells with muscarinic agonists leads to the ERK1/2-dependent phosphorylation and activation of p90RSK (Cheng et al., 2003; Cheng and Raufman; 2005), a nuclear response protein that represents a key regulator of gene expression and cell cycle progression (Anjum and Blenis, 2008). It is therefore likely that M3R-mediated activation of p90RSK is intimately linked to muscarinic agonist-induced H508 cell proliferation (Cheng et al., 2003; Cheng and Raufman; 2005). Consistent with previous reports, we found that carbachol (500 μ M) treatment of H508 cells electroporated with control siRNA stimulated the phosphorylation of p90RSK (Fig. 10). Interestingly, carbachol-induced phosphorylation of p90RSK was significantly more pronounced in cells that had been treated with Tmem147 siRNA ($p < 0.05$; Fig. 10).

To examine the effect of siRNA-mediated knockdown of Tmem147 expression on cell surface M3R expression levels in H508 cells, we carried out [3 H]NMS binding studies with intact H508 cells (note that [3 H]NMS is unable to cross the plasma membrane). We found that siRNA-mediated silencing of Tmem147 expression led to a 1.99 (\pm 0.20)-fold increase ($p < 0.05$) in the number of cell surface M3Rs, as compared with cells treated with control siRNA (number of [3 H]NMS binding sites per μ g H508

MOL #67363

cell protein obtained with control samples: $1.21 \pm 0.17 \times 10^6$; $n=4$; assays were carried out at the end of the 5-day incubation period with carbachol medium). To label both cell surface M3Rs as well as M3Rs located in intracellular compartments, we carried out analogous studies using [^3H]QNB, a membrane-permeable muscarinic radioligand. Using control siRNA-treated cells, we found that [^3H]QNB labeled ~3-4-fold more M3Rs than [^3H]NMS (number of [^3H]QNB binding sites per μg H508 cell protein obtained with control samples: $4.10 \pm 0.60 \times 10^6$; $n=2$), indicating that a major portion of M3Rs is retained intracellularly under the chosen experimental conditions. siRNA-mediated silencing of Tmem147 expression led to a $1.93 (\pm 0.16)$ -fold increase in the number of [^3H]QNB binding sites, a value that was not significantly different from that found in the [^3H]NMS binding studies (see above). These observations suggest that the increase in cell surface M3R expression observed after knockdown of Tmem147 expression is largely due to an increase in the total amount of correctly folded M3Rs and that the Tmem147/M3R interaction interferes with the proper folding of the receptor protein.

Co-expression of M3R and Tmem147 Transcripts in Several Mouse Tissues. To examine whether Tmem147 transcripts could be detected in tissues where the M3R is known to be expressed physiologically, we subjected total RNA prepared from several mouse tissues to RT-PCR analysis. Using gene-specific primer pairs, we found that M3R and Tmem147 transcripts were co-expressed in all analyzed mouse tissues, including cerebral cortex, submandibular gland, hypothalamus, pancreas, liver, and ileum (Fig. 11).

Discussion

In this study, we used the full-length M3R as a bait in a split ubiquitin MbYTH screen to identify novel M3R-interacting proteins. This strategy led to the recovery of many proteins that were able to interact with the M3R in yeast. Interestingly, one full-length protein, Tmem147, was recovered 11 independent times in this screen. Tmem147 is an integral membrane protein of unknown function that is widely expressed in many peripheral and central tissues. The amino acid sequence of Tmem147 is highly conserved (~99%) among mammals, suggesting that Tmem147 may have important physiological functions. Consistent with the M3R/Tmem147 interaction observed in yeast, we demonstrated that M3R and Tmem147 transcripts were co-expressed in several mouse tissues where the M3R is known to be expressed physiologically.

Confocal microscopic studies demonstrated that Tmem147 is an ER-membrane-associated protein. Interestingly, overexpression of Tmem147 in COS-7 cells led to the intracellular retention of the M3R in the ER, suggesting that Tmem147 regulates the transport of the M3R to the cell surface.

Similar to Tmem147, several other proteins have been identified that can regulate the cell surface expression of certain GPCRs. For example, Bermak et al. (2001) found that DRiP78, an ER-membrane-associated protein, can interact with the D1 dopamine receptor, leading to its retention in the ER. Moreover, several chaperones and other escort proteins have been shown to promote cell surface expression of certain GPCRs (Ritter and Hall, 2009). Interestingly, heterodimer formation between the GABA_B-1 and -2

MOL #67363

receptor subtypes is required for efficient trafficking of GABA_B receptors to the cell surface (Jones et al., 1998).

Consistent with the M3R/Tmem147 interaction observed in yeast, co-immunoprecipitation studies demonstrated that the M3R was also associated with Tmem147 in co-transfected mammalian cells (COS-7 cells). In agreement with the observation that Tmem147 impairs exit of the M3R from the ER, the number of detectable [³H]NMS binding sites was drastically reduced in COS-7 cells co-expressing the M3R and Tmem147. Tmem147 co-expression also led to reduced M3R-mediated calcium mobilization, probably as a consequence of reduced M3R cell surface expression. Preliminary studies demonstrated that other class I GPCRs, including the M₁ muscarinic and the V₂ vasopressin receptor subtypes could also be co-immunoprecipitated with Tmem147 in co-transfected COS-7 cells. It is therefore likely that Tmem147 also regulates the expression and function of other (non-M3R) GPCRs.

Several recent DNA microarray studies have shown that the expression of the Tmem147 gene (NIFIE14) is upregulated in various human cancers (Basil et al., 2006; Staub et al., 2007; Velazquez et al., 2007), raising the possibility that Tmem147 may play a role tumor formation. In addition, a considerable body of evidence suggests that enhanced M3R activity may contribute to the pathogenesis of colon cancers (Frucht et al., 1999; Cheng et al., 2003; Cheng and Raufman; 2005; Raufman et al., 2008; Xie et al., 2009). For example, Raufman et al. (2008) recently demonstrated that azoxymethane treatment caused significantly fewer colon tumors in M3R knockout mice than in WT littermates. On the basis of these findings, we decided to explore the possible

MOL #67363

physiological significance of the M3R/Tmem147 interaction in the H508 colon tumor cell line.

H508 cells are known to express M3Rs endogenously (Frucht et al, 1999). We demonstrated that the M3R is the only muscarinic receptor subtype that is expressed at significant levels in this cell line. In agreement with previous findings, we demonstrated that the hydrolytically stable muscarinic agonist, carbachol, promoted H508 cell proliferation and the phosphorylation of p90RSK. Previous studies also suggest that M3R-mediated activation of p90RSK is intimately linked to carbachol-induced H508 cell proliferation (Cheng et al., 2003; Cheng and Raufman, 2005). Strikingly, siRNA-mediated knockdown of Tmem147 expression in H508 cells led to a significant increase in carbachol-promoted cell proliferation and p90RSK phosphorylation. Knockdown of Tmem147 expression was also associated with a significant increase in the number of M3Rs present on the cell surface, as determined in [³H]NMS radioligand binding studies carried out with intact H508 cells. Taken together, these findings provide convincing evidence that endogenous Tmem147 also regulates the activity of M3Rs endogenously expressed by a colon cancer cell line. It is therefore highly likely that the Tmem147/M3R interaction is also of physiological relevance.

In future studies, we are planning to identify the structural elements that are critical for the observed Tmem147/M3R interaction. These studies should also provide more detailed mechanistic insight into how Tmem147 binding leads to M3R retention in the ER.

After completion of this study, Jin et al. (2010) reported the usefulness of the split ubiquitin two-hybrid screen to identify proteins that can associate with the μ -opioid

MOL #67363

receptor (MOR). Specially, the authors identified GPR177, the mammalian ortholog of *Drosophila* Wntless, as a novel MOR-interacting protein. Additional experiments indicated that morphine treatment led to enhanced MOR/GPR177 complex formation at the cell periphery and inhibition of Wnt protein secretion, perhaps resulting in decreased neurogenesis (Jin et al., 2010).

In conclusion, these results demonstrate that the split ubiquitin two-hybrid screen (MbYTH screen) represents a powerful approach to identify novel GPCR-interacting proteins. In the present study, we used this strategy to identify many novel M3R-associated proteins, including Tmem147, an ER resident protein. Since the vast majority of these proteins were not detected in conventional YTH screens, it is likely that most of the M3R-associated proteins that emerged from the MbYTH screen require the presence of the membrane-embedded full-length M3R for high affinity binding. Since M3R-dependent signaling pathways are involved in many important physiological and pathophysiological processes, Tmem147 and other M3R-associated proteins may represent novel targets for modulating M3R activity for therapeutic purposes.

MOL #67363

Acknowledgments

We thank Drs. Jean-Pierre Raufman and Kunrong Cheng (University of Maryland School of Medicine, Baltimore) for advice and helpful discussions regarding the H508 cell assays.

Authorship contributions

Participated in research design: Rosemond, Rossi, McMillin, Scarselli, and Wess.

Conducted experiments: Rosemond, Rossi, McMillin, and Scarselli.

Performed data analysis: Rosemond, Rossi, McMillin, Scarselli, and Donaldson.

Wrote or contributed to the writing of the manuscript: Rosemond, and Wess.

MOL #67363

References

- Anjum R and Blenis J (2008) The RSK family of kinases: emerging roles in cellular signalling. *Nat Rev Mol Cell Biol* **9**:747-758.
- Basil CF, Zhao Y, Zavaglia K, Jin P, Panelli MC, Voiculescu S, Mandruzzato S, Lee HM, Seliger B, Freedman RS, et al. (2006) *Cancer Res* **66**:2953-2961.
- Bermak JC, Li M, Bullock C, and Zhou QY (2001) Regulation of transport of the dopamine D1 receptor by a new membrane-associated ER protein. *Nat Cell Biol* **3**:492-498
- Bockaert J, Perroy J, Bécamel C, Marin P, and Fagni L (2010) GPCR interacting proteins (GIPs) in the nervous system: Roles in physiology and pathologies. *Annu Rev Pharmacol Toxicol* **50**:89-109.
- Caulfield MP and Birdsall NJM (1998) International Union of Pharmacology XVII Classification of muscarinic acetylcholine receptors *Pharmacol Rev* **50**:279-290
- Cheng K and Raufman JP (2005) Bile acid-induced proliferation of a human colon cancer cell line is mediated by transactivation of epidermal growth factor receptors. *Biochem Pharmacol* **70**:1035-1047.
- Cheng K, Xie G, and Raufman J-P (2007) Matrix metalloproteinase-7-catalyzed release of HB-EGF mediates deoxycholytaurine-induced proliferation of a human colon cancer cell line. *Biochem Pharmacol* **73**:1001-1012.
- Cheng K, Zimniak P, and Raufman JP (2003) Transactivation of the epidermal growth factor receptor mediates cholinergic agonist-induced proliferation of H508 human colon cancer cells. *Cancer Res* **63**:6744-6750.
- Eglen RM (2005) Muscarinic receptor subtype pharmacology and physiology. *Prog Med Chem* **43**:105-136.
- Erlenbach I, Kostenis E, Schmidt C, Hamdan FF, Pausch MH, and Wess J (2001) Functional expression of M₁, M₃ and M₅ muscarinic acetylcholine receptors in yeast. *J Neurochem* **77**:1327-1337
- Free RB, Hazelwood LA, Cabrera DM, Spalding HN, Namkung Y, Rankin ML, and Sibley DR (2007) D₁ and D₂ dopamine receptor expression is regulated by direct interaction with the chaperone protein calnexin. *J Biol Chem* **282**:21285-21300.

MOL #67363

- Frucht H, Jensen RT, Dexter D, Yang WL, and Xiao Y (1999) Human colon cancer cell proliferation mediated by the M₃ muscarinic cholinergic receptor. *Clin Cancer Res* **5**:2532-2539.
- Gautam D, Han SJ, Hamdan FF, Jeon J, Li B, Li JH, Cui Y, Mears D, Lu H, Deng C, et al. (2006) A critical role for β cell M₃ muscarinic acetylcholine receptors in regulating insulin release and blood glucose homeostasis in vivo. *Cell Metab* **3**:449-461.
- Gautam D, Jeon J, Starost MF, Han SJ, Hamdan FF, Cui Y, Parlow AF, Gavrilova O, Szalayova I, Mezey E, and Wess J (2009) Neuronal M₃ muscarinic acetylcholine receptors are essential for somatotroph proliferation and normal somatic growth. *Proc Natl Acad Sci USA* **106**:6398-6403.
- Goin JC and Nathanson NM (2006) Quantitative analysis of muscarinic acetylcholine receptor homo- and heterodimerization in live cells: regulation of receptor down-regulation by heterodimerization. *J Biol Chem* **281**:5416-5425.
- Iyer K, Bürkle L, Auerbach D, Thaminy S, Dinkel M, Engels K, and Stagljar I (2005) Utilizing the split-ubiquitin membrane yeast two-hybrid system to identify protein-protein interactions of integral membrane proteins. *Sci STKE* **275**:13.
- Jin J, Kittanakom S, Wong V, Reyes BA, Van Bockstaele EJ, Stagljar I, Berrettini W, and Levenson R (2010) Interaction of the mu-opioid receptor with GPR177 (Wntless) inhibits Wnt secretion: potential implications for opioid dependence. *BMC Neurosci* **11**:33.
- Jones KA, Borowsky B, Tamm JA, Craig DA, Durkin MM, Dai M, Yao WJ, Johnson M, Gunwaldsen C, Huang LY, et al. (1998) GABA_B receptors function as a heteromeric assembly of the subunits GABA_BR1 and GABA_BR2. *Nature* **396**:674-679.
- Kittanakom S, Chuk M, Wong V, Snyder J, Edmonds D, Lydakis A, Zhang Z, Auerbach D, and Stagljar I (2009) Analysis of membrane protein complexes using the split-ubiquitin membrane yeast two-hybrid (MYTH) system. *Methods Mol Biol* **548**:247-271.
- Li JH, Gautam D, Han SJ, Guettier JM, Cui Y, Lu H, Deng C, O'Hare J, Jou W, Gavrilova O, Buettner C, and Wess J (2009) Hepatic muscarinic acetylcholine receptors are not critically involved in maintaining glucose homeostasis in mice. *Diabetes* **58**:2776-2787.

MOL #67363

- Lucas JL, Wang D, and Sadée W (2006) Calmodulin binding to peptides derived from the i3 loop of muscarinic receptors. *Pharm Res* **23**:647-653.
- Mitchell R, Robertson DN, Holland PJ, Collins D, Lutz EM, and Johnson MS (2003) ADP-ribosylation factor-dependent phospholipase D activation by the M3 muscarinic receptor. *J Biol Chem* **278**:33818-33830.
- Mumberg D, Müller R, and Funk M (1995) Yeast vectors for the controlled expression of heterologous proteins in different genetic backgrounds. *Gene* **156**:119-122.
- Pausch MH, Price LA, Kajkowski EM, Strnad J, dela Cruz F, Heinrich J, Ozenberger BA, and Hadcock JR (1998) Heterologous G protein-coupled receptors expressed in *Saccharomyces cerevisiae*: Methods for genetic analysis and ligand identification, in Identification and Expression of G Protein-Coupled Receptors (Lynch KR ed) pp 196-212, Wiley-Liss, New York.
- Raufman JP, Samimi R, Shah N, Khurana S, Shant J, Drachenberg C, Xie G, Wess J, and Cheng K (2008) Genetic ablation of M₃ muscarinic receptors attenuates murine colon epithelial cell proliferation and neoplasia. *Cancer Res* **68**:3573-3578.
- Ritter SL and Hall RA (2009) Fine-tuning of GPCR activity by receptor-interacting proteins. *Nat Rev Mol Cell Biol* **10**:819-830.
- Scarselli M and Donaldson JG (2009) Constitutive internalization of G protein-coupled receptors and G proteins via clathrin-independent endocytosis. *J Biol Chem* **284**:3577-3585.
- Scarselli M, Li B, Kim SK, and Wess J (2007) Multiple residues in the second extracellular loop are critical for M₃ muscarinic acetylcholine receptor activation. *J Biol Chem* **282**:7385-7396.
- Schöneberg T, Liu J, and Wess J (1995) Plasma membrane localization and functional rescue of truncated forms of a G protein-coupled receptor. *J Biol Chem* **270**:18000-18006.
- Schöneberg T, Yun J, Wenkert D, and Wess J (1996) Functional rescue of mutant V2 vasopressin receptors causing nephrogenic diabetes insipidus by a co-expressed receptor polypeptide. *EMBO J* **15**:1283-1291.

MOL #67363

- Shi Y, Oury F, Yadav VK, Wess J, Liu XS, Guo XE, Murshed M, and Karsenty G (2010) Signaling through the M₃ muscarinic receptor favors bone mass accrual by decreasing sympathetic activity. *Cell Metab* **11**:231-238.
- Skehan P, Storeg R, Scudiero D, Monks A, McMahon J, Vistica D, Warren JT, Bokesch H, Kenney S, and Boyd MR (1990) New colorimetric cytotoxicity assay for anticancer-drug screening. *J Natl Cancer Inst* **82**:1107-1112.
- Stagljär I and Fields S (2002) Analysis of membrane protein interactions using yeast-based technologies. *Trends Biochem Sci* **27**:559-563.
- Stagljär I, Korostensky C, Johnsson N, and te Heesen S (1998) A genetic system based on split-ubiquitin for the analysis of interactions between membrane proteins in vivo. *Proc Natl Acad Sci USA* **95**:5187-5192.
- Staub E, Groene J, Heinze M, Mennerich D, Roepcke S, Klamann I, Hinzmann B, Castanos-Velez E, Pilarsky C, Mann B, Brümmendorf T, et al. (2007) Genome-wide expression patterns of invasion front, inner tumor mass and surrounding normal epithelium of colorectal tumors. *Mol Cancer* **6**:79.
- Velazquez EF, Yancovitz M, Pavlick A, Berman R, Shapiro R, Bogunovic D, O'Neill D, Yu YL, Spira J, Christos PJ, et al. (2007) Clinical relevance of neutral endopeptidase (NEP/CD10) in melanoma. *J Transl Med* **5**:2.
- Wess J (1996) Molecular biology of muscarinic acetylcholine receptors *Crit Rev Neurobiol* **10**:69-99.
- Wess J, Eglen RM, and Gautam D (2007) Muscarinic acetylcholine receptors: mutant mice provide new insights for drug development. *Nat Rev Drug Discov* **6**:721-733.
- Xie G, Cheng K, Shant J, and Raufman JP (2009) Acetylcholine-induced activation of M₃ muscarinic receptors stimulates robust matrix metalloproteinase gene expression in human colon cancer cells. *Am J Physiol Gastrointest Liver Physiol* **296**:G755-763.
- Zeng FY and Wess J (1999) Identification and molecular characterization of m3 muscarinic receptor dimers. *J Biol Chem* **274**:19487-19497.

MOL #67363

Footnote

This research was supported by the Intramural Research Program of the NIH, NIDDK
(Bethesda, Maryland).

Figure Legends

Fig. 1. Scheme of the membrane-based yeast two-hybrid (MbYTH) screen used in the present study. To obtain a bait for the MbYTH screen, we first generated a modified version of the rat M3R (M3-Cub) fused at its C-terminus to the Cub domain (C-terminal portion of ubiquitin) and an artificial transcription factor (TF; Stagljar and Fields, 2002; Iyer et al., 2005; Kittanakom et al., 2009). Potential M3-Cub-interacting proteins (preys) were expressed by a human brain cDNA library coding for proteins containing an N-terminal Nub tag (N-terminal portion of ubiquitin). The prey can be a cytosolic protein or a membrane protein with an N-terminus that is located in the cytoplasm. To decrease the likelihood of spontaneous interactions between the Nub and Cub domains, an I->G point mutation was introduced into the Nub domain (NubG; Stagljar and Fields, 2002; Iyer et al., 2005; Kittanakom et al., 2009). As a result, NubG will only efficiently interact with Cub when the two proteins to which the two tags are attached interact with each other, resulting in the formation of a NubG-Cub complex. This complex is recognized by ubiquitin-specific proteases (UBPs) which release the artificial TF from the M3-Cub construct. The TF then enters the nucleus via diffusion and binds to the lexA-binding sites upstream of the *HIS3*, *ADE2*, and *LacZ* reporter genes. Activation of the *HIS3* gene allows for yeast growth in histidine-deficient media. The *LacZ* reporter provides for the colorimetric detection of Gal4p activity.

Fig. 2. Carbachol-induced yeast growth mediated by activation of WT-M3 or M3-Cub receptors. The indicated receptors were expressed in the MPY578q5 yeast strain

MOL #67363

expressing a hybrid chimeric yeast/mammalian G protein α subunit (for details, see Materials and Methods). Yeast growth was measured by determining the absorbance at 630 nm, either in the absence or presence of increasing concentrations of the muscarinic agonist, carbachol. The curves shown are representative of three independent experiments, each carried out in triplicate. Data are given as means \pm S.E.M.

Fig. 3. Yeast growth assay used to establish optimal conditions for the planned MbYTH screen. The pAMBV4-M3-Cub plasmid was transformed into the NMY51 yeast strain, together with the indicated control plasmids (Alg5-NubI, Alg5-NubG, or pADL-Nx [empty vector]). Yeast growth was measured by determining the absorbance at 630 nm. The compositions of the media used are indicated in the inset. Yeast growth was determined in the absence or presence of the indicated concentrations of 3-AT, an agent that blocks one of the key enzymes involved in histidine biosynthesis. The data shown are representative of three independent experiments, each carried out in triplicate.

Fig. 4. Co-immunoprecipitation of Tmem147 with M3Rs in co-transfected COS-7 cells. The Tmem147 construct that was used for co-immunoprecipitation studies contained an N-terminal FLAG epitope tag (Tmem147-FLAG). Similarly, the M3R construct used (human) contained three consecutive HA epitopes at its N-terminus (M3R-HA). Membranes prepared from COS-7 cells that had been co-transfected with the two constructs were solubilized, and proteins were immunoprecipitated with the indicated antibodies. Immunoprecipitates were analyzed via Western blotting using an anti-FLAG (left panel) or an anti-HA antibody, respectively. Lanes 2, 3, 5, and 6 show the results

MOL #67363

obtained with cells co-expressing Tmem147-FLAG and M3R-HA. Lanes 1 and 4 show the results of control experiments in which membranes were prepared from COS-7 cells expressing either Tmem147-FLAG or M3R-HA and then mixed. In mock IP experiments, cell lysates were incubated with protein-A agarose in the absence of antibodies.

Fig. 5. Tmem147 is found in the ER of transfected COS-7 cells. The subcellular localization of Tmem147 was studied via confocal microscopy using COS-7 cells transiently expressing Tmem147-FLAG. A, Tmem147 is localized to the ER (pDsRed2-ER represents an ER-specific marker; Free et al., 2007). B, C, Tmem147 is not present in the Golgi (GM130 is a Golgi marker protein) or in early endosomes (EEA1 is a marker protein for early endosomes). All studies were carried out with cells permeabilized with 0.2% saponin. To visualize Tmem147-FLAG, Alexa-594- (red) or Alexa-488-conjugated (green) secondary antibodies were used in panels (B) and (C) respectively (after incubation with a polyclonal anti-FLAG antibody). For experimental details, see Materials and Methods.

Fig. 6. Effect of Tmem147 expression on the subcellular distribution of the M3R in co-transfected COS-7 Cells. The subcellular localization of the M3R-HA receptor, either expressed alone or co-expressed with Tmem147-FLAG was studied via confocal microscopy using transfected COS-7 cells. After fixation, cells were permeabilized with 0.2% saponin. A, Transfection with the M3R-HA construct alone. Cells were stained with a monoclonal anti-HA antibody followed by incubation with a secondary antibody. Note

MOL #67363

the intense staining of the M3R-HA protein on the cell surface. B, Transfection with vector DNA (pcDNA3.1; control). Cells were treated with the anti-HA antibody to reveal background staining. C, Transfection with the Tmem147-FLAG construct alone. Tmem147-FLAG was visualized by using a polyclonal anti-FLAG antibody followed by incubation with a secondary antibody. Note that Tmem147 protein was retained intracellularly (in the ER; see Fig. 5). D- F, Co-transfection of COS-7 cells with the M3R-HA and Tmem147-FLAG constructs. Cells were stained with the indicated antibodies. Note that cell surface expression of the M3R-HA receptor was barely visible in the presence of co-expressed Tmem147-FLAG (D) and that the two proteins were co-localized in the ER (D-F). For experimental details, see Materials and Methods.

Fig. 7. Effect of Tmem147 on M3R expression levels and M3R-mediated calcium responses in co-transfected COS-7 cells. A, Effect of Tmem147 expression on M3R receptor expression levels (B_{\max}), as determined in [^3H]NMS saturation binding assays. B, Effect of Tmem147 expression on M3R-mediated calcium responses. Carbachol-induced increases in intracellular calcium levels were measured by using FLIPR technology. All experiments were carried out using COS-7 cells that had been cotransfected with plasmids coding for the human M3R and Tmem147 (see Materials and Methods for details). Data are presented means \pm S.E.M. of three independent experiments carried out in duplicate. RFU, relative fluorescence units.

Fig. 8. Determination of gene expression levels in H508 cells using real-time qRT-PCR. A, M_1 - M_5 muscarinic receptor mRNA levels in H508 cells. Muscarinic receptor

MOL #67363

transcript levels were determined by real-time qRT-PCR using total RNA prepared from H508 cells. Data are expressed relative to M3R mRNA levels (=100%). B, Knockdown of Tmem147 expression following treatment of H508 cells with Tmem147 siRNA. Cells were treated with negative control siRNA or Tmem147 siRNA, as described under Materials and Methods. Data are expressed relative to mRNA levels observed with cells treated with negative control siRNA (=100%). Primer sequences are given under Materials and Methods. Data are presented as means \pm S.E.M. of three independent experiments carried out in triplicate.

Fig. 9. Effect of siRNA-mediated knock-down of Tmem147 expression on the M3R-mediated increase in H508 cell proliferation. Cells were treated with negative control siRNA or Tmem147 siRNA, as described in detail under Materials and Methods. Cells were grown for 5 days in the absence or presence of the muscarinic agonist, carbachol (100 μ M), either in the absence or presence of the muscarinic antagonist, atropine (1 μ M). Cell growth was determined by using a colorimetric assay (see Materials and Methods for details). In each individual experiment, cell growth observed with cells that had been treated with control siRNA and had not been exposed to carbachol was set equal to 100%. Results are expressed as means \pm S.E.M. of four separate experiments (* p < 0.05).

Fig. 10. Effect of siRNA-mediated knock-down of Tmem147 expression in H508 cells on M3R-mediated increases in the expression of phosphorylated p90RSK (P-p90RSK). Cells were treated with negative control siRNA (Con) or Tmem147 siRNA (147) and grown in

MOL #67363

carbachol medium for 5 days, as described in detail under Materials and Methods. Cells were then acutely stimulated with 500 μ M of carbachol for 10 min. A, Representative Western blot. B, Summary of two or three separate immunoblotting experiments. P-p90RSK expression levels are expressed as means \pm S.E.M. relative to the levels determined with cells that had been electroporated with negative control siRNA and had not been treated with 500 μ M of carbachol (= 100%; * p < 0.05).

Fig. 11. Co-expression of M3R and Tmem147 transcripts in several mouse tissues.

Total RNA was prepared from the indicated mouse tissues (C57BL/6NTac mice). RT-PCR studies were carried out as described under Materials and Methods, using gene-specific primer pairs (M3R, top panel; Tmem147, lower panel). The sizes of the PCR products were: M3R, 158 bp; Tmem147, 156 bp. RT, reverse transcriptase; C. cortex, cerebral cortex; Subm. gland, submandibular gland.

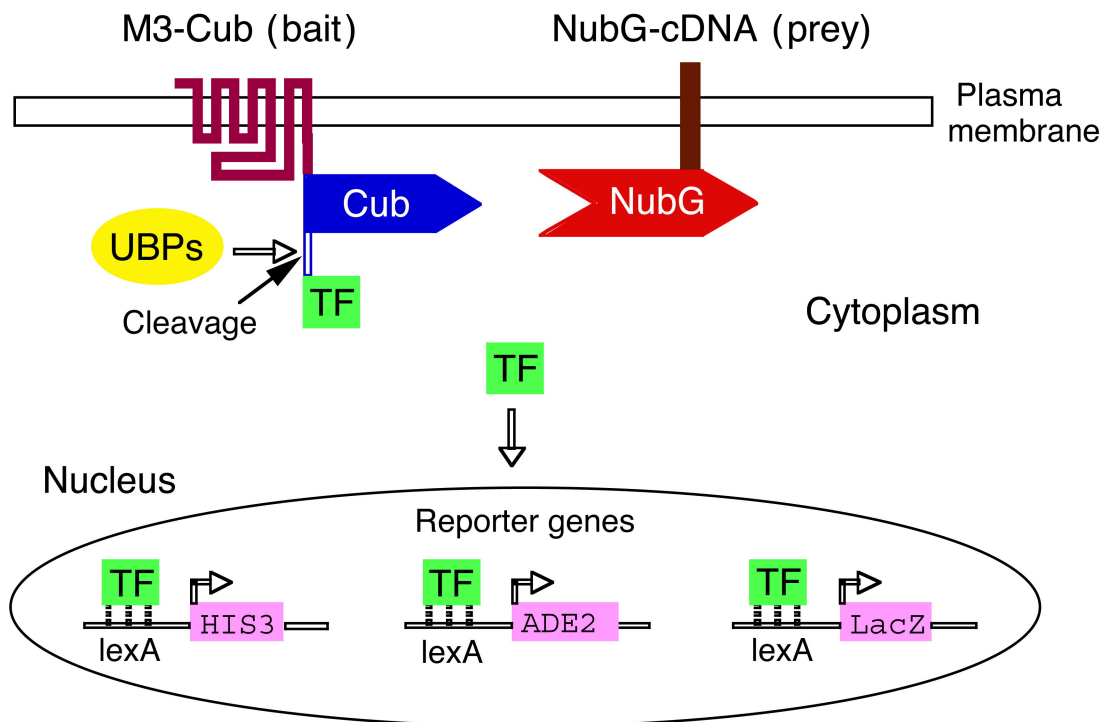


Fig. 1

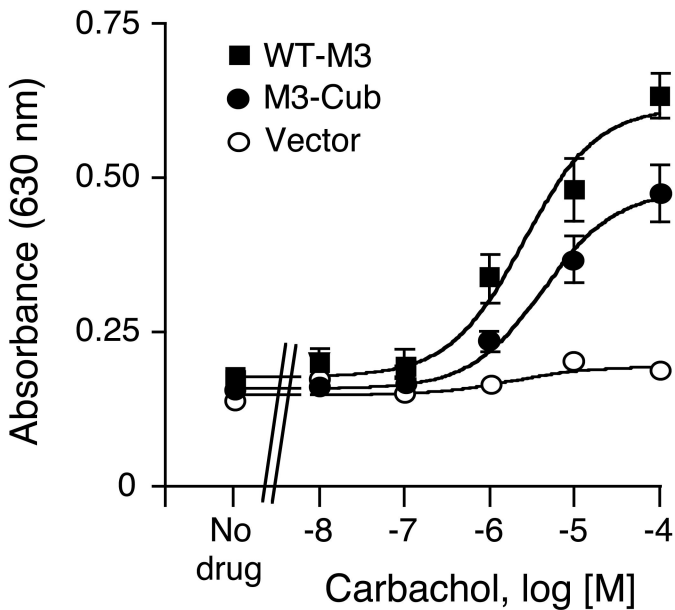
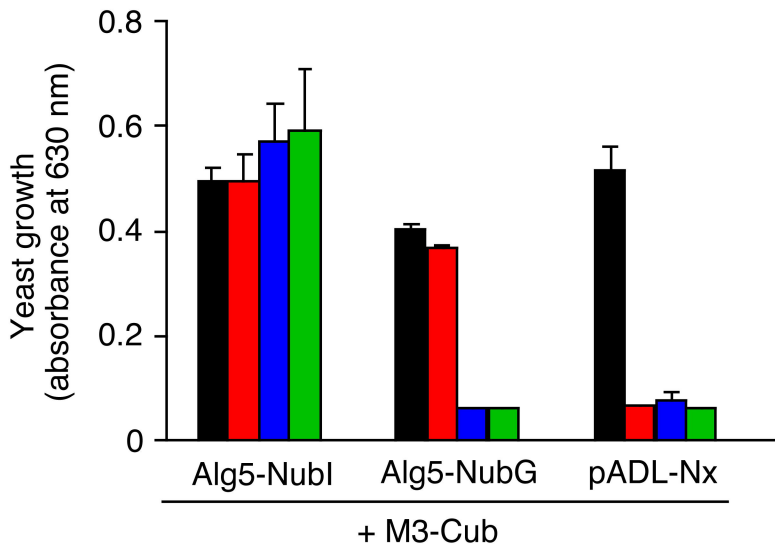


Fig. 2



Growth conditions

- leu-trp
- leu-trp-his-ade
- leu-trp-his-ade (+ 10 mM 3-AT)
- leu-trp-his-ade (+ 25 mM 3-AT)

Fig. 3

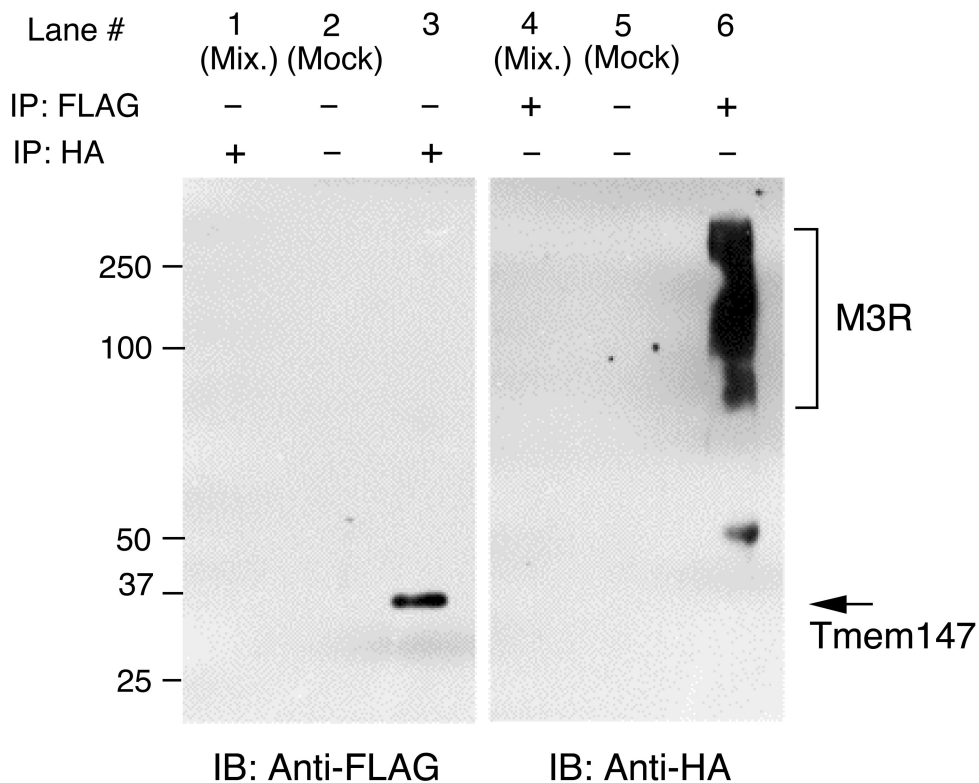
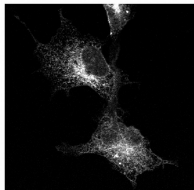
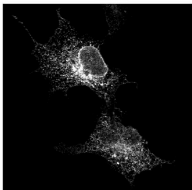


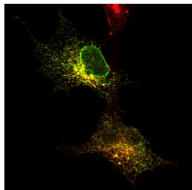
Fig. 4

A

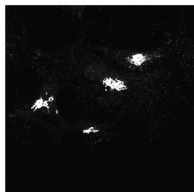
pDsRed2-ER



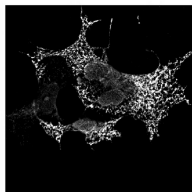
Tmem147 (FLAG)



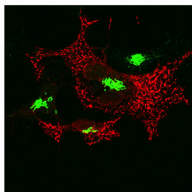
Merged

B

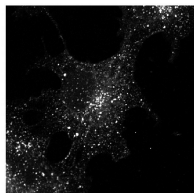
anti-GM130



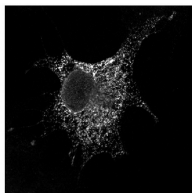
Tmem147 (FLAG)



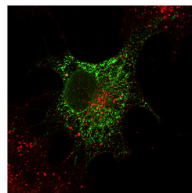
Merged

C

anti-EEA1

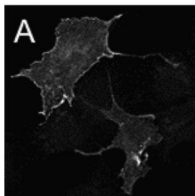


Tmem147 (FLAG)

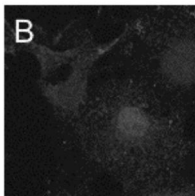


Merged

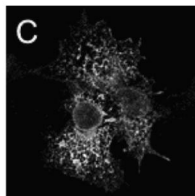
Fig. 5



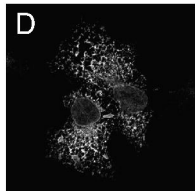
M3R total (HA)



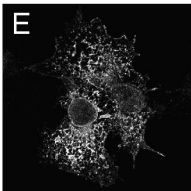
Vector



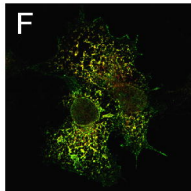
Tmem147 total (FLAG)



M3R total (HA)



Tmem147 total (FLAG)



Merged

Fig. 6

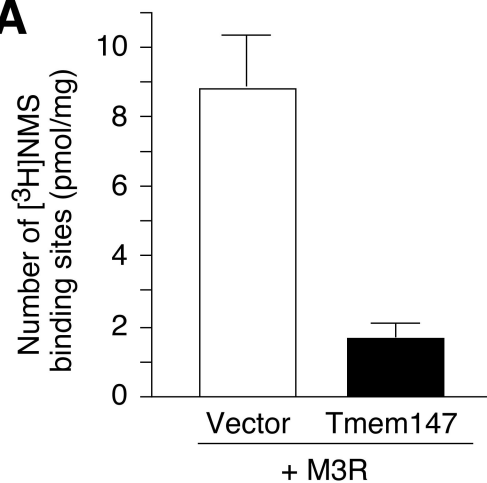
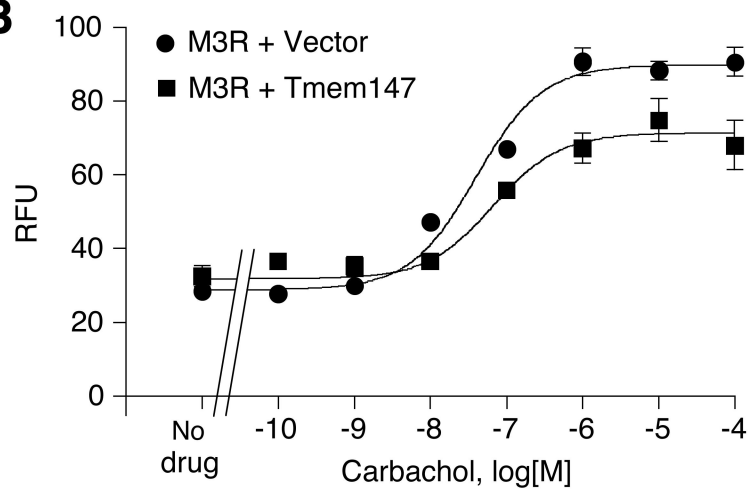
A**B**

Fig. 7

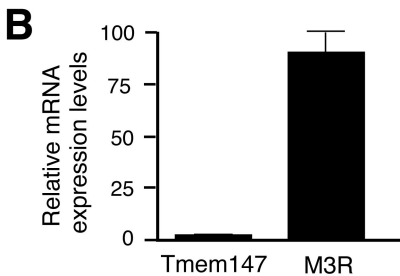
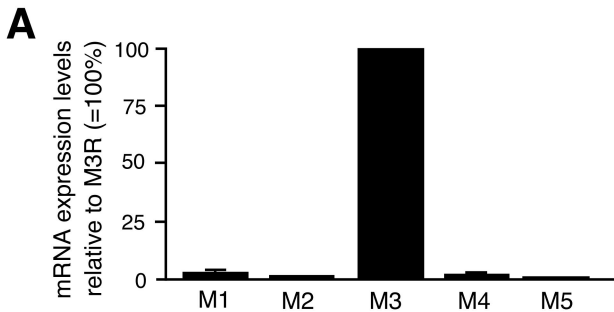


Fig. 8

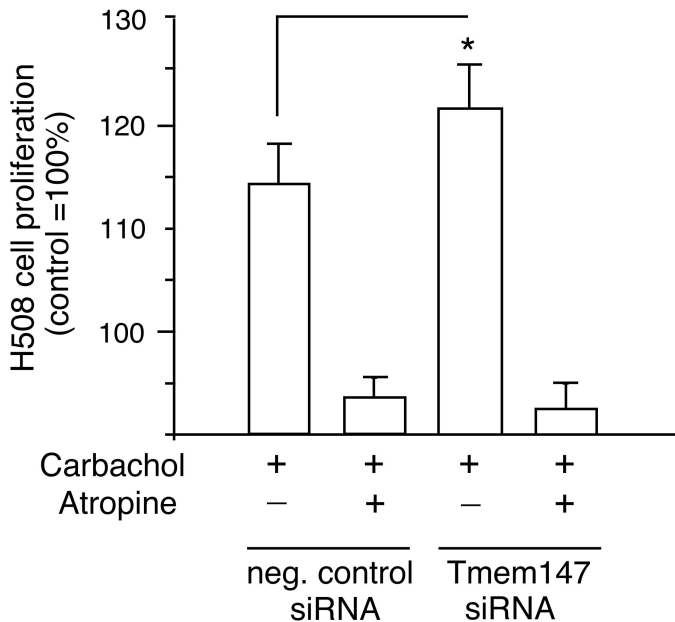


Fig. 9

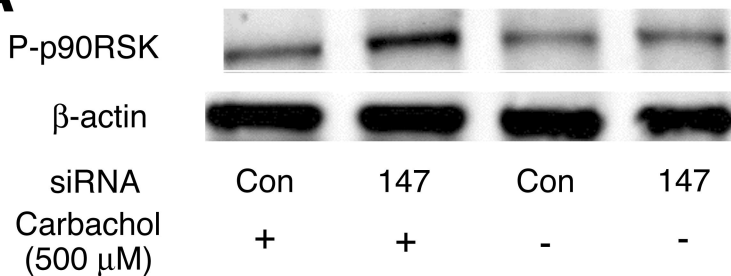
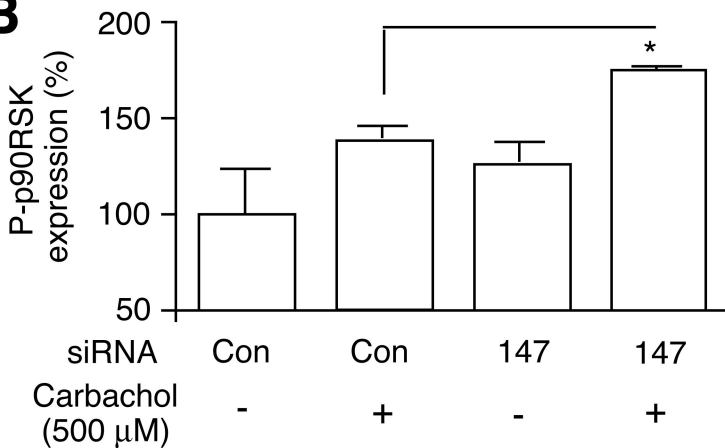
A**B**

Fig. 10

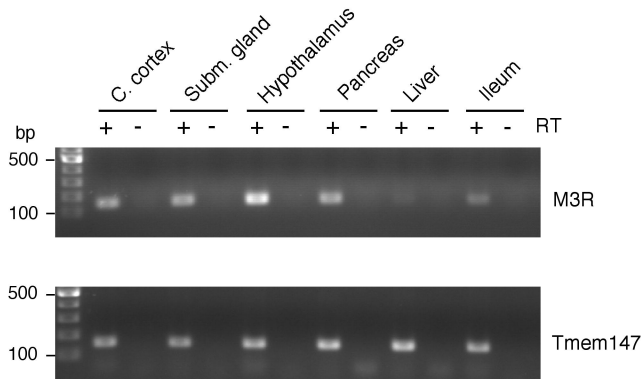


Fig. 11

Supplemental Data

Regulation of M₃ Muscarinic Receptor Expression and Function by Transmembrane
Protein 147

Erica Rosemond, Mario Rossi, Sara M. McMillin, Marco Scarselli, Julie G. Donaldson,
and Jürgen Wess

Supplemental Table 1

M3R-interacting proteins identified in a membrane-based yeast two-hybrid screen

Protein	Accession No.
Tetraspanin family	
CD82	AAB23825
CD9	P21926
CD63	AAV38940
Ubiquitin-associated proteins	
Small ubiquitin-related modifier 2 precursor (SUMO-1)	AAC50996
Small ubiquitin-related modifier 2 precursor (SUMO-2)	P61956
UBC protein	AAH08955
Ubiquitin C	NP_066289
Receptor proteins/Transmembrane proteins	
Transmembrane protein 147	AAH01118 / BC001118
G protein-coupled receptor 37	NP_005293
Homo sapiens G protein-coupled receptor, family C, group 5, member B (GPC5B)	NM_016235 / AAF05331
Rhodopsin	NP_000530
Aquaporin-4 (AQP-4)	P55087
Glutamate receptor, ionotropic, N-methyl D-aspartate-associated protein 1	NP_001009184
Sodium channel, voltage gated, type VIII, alpha	NP_055006
Transmembrane 9 superfamily member 2	CAH71381
Transmembrane protein 14A	AAH19328
Signaling molecules	
Phosphatidic acid phosphatase type 2C	AAP35667
Calmodulin 2	AAH08437
Protein kinase Njmu-R1	AAH54035
2',3'-Cyclic nucleotide 3' phosphodiesterase (CNP)	AAH06392
Solute carrier proteins	
Solute carrier family 39 (zinc transporter), member 3 isoform a	NP_653165
Solute carrier family 22 (organic cation transporter), member 17 isoform b	NP_057693
Solute carrier family 31 (copper transporters), member 2	NP_001851
Solute carrier family 35, member B1	NP_005818
FXD domain-containing ion transport regulator 6	NP_071286

PLP domain-containing proteins

Glycoprotein M6B isoform 1 variant	BAD92762
Proteolipid protein 1 (Pelizaeus-Merzbacher disease, spastic paraplegia 2, uncomplicated)	CAA98191

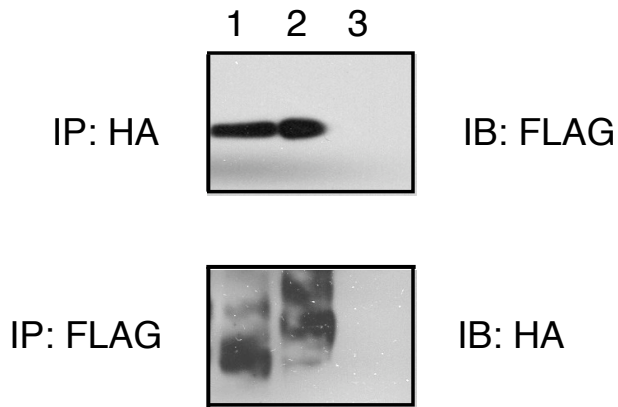
Signal sequence proteins

Homo sapiens signal sequence receptor, gamma (translocon-associated protein gamma) [synthetic construct]	AAP36250
Signal sequence receptor gamma subunit	AAH17203
Signal peptidase complex subunit 1 homolog	NP_054760
Signal peptidase 12 kDa subunit	AAL31361

Other proteins

Nogo-A protein short form	AAG40878
LAG1 longevity assurance homolog 2, isoform 1	AAH10032
FLJ20489 protein	AAH65033
Yip1 domain family, member 6	NP_776195
HCV F-transactivated protein 1	AAT35812
BCL2/adenovirus E1B 19kDa interacting protein 3-like	AAV38308
Growth-inhibiting gene 5 protein	AAS00486
B-cell receptor-associated protein 31 variant (BAP31)	BAD96214
Delta-notch-like EGF repeat-containing transmembrane	NP_620711
Claudin 5	AAP35918
Immediate early response 3 interacting protein 1	NP_057181
BAX inhibitor 1	AAU29521
Tumor differentially expressed protein 1 variant	BAD96643
HSPC288	AAF28966
Leptin receptor overlapping transcript-like 1	AAH00642
Interferon induced transmembrane protein 1	AAH00897
Homolog of yeast long chain polyunsaturated fatty acid elongation	AAH67123
BM88 antigen	AAH34732
Thymopoietin isoform gamma	NP_001027455
Myelin and lymphocyte protein (T-lymphocyte maturation-associated protein)	P21145
Ovarian carcinoma immunoreactive antigen	AAG45220
Syntaxin 8	NP_004844
ZMYM6 protein	AAH29439
β -amyloid precursor-like protein 2 (APLP-2)	AAA35526
Prostaglandin D2 synthase 21kDa	CAI12758
Intercellular adhesion molecule 2 precursor variant	BAD93115
Thymic dendritic cell-derived factor 1	AAH16374
NADH dehydrogenase subunit 4	ABB91083
NADH dehydrogenase subunit 4L	AAX53836
Lysosomal-associated protein transmembrane 4 alpha	AAH00421
Sterol-C4-methyl oxidase-like isoform 1	NP_006736

Dolichyl-phosphate mannosyltransferase polypeptide 2, regulatory subunit, isoform 1	AAH15233
Histone deacetylase-like protein	CAA09893
ATP synthase, H ⁺ transporting, mitochondrial F0 complex, subunit	AAI06882
ATPase, H ⁺ transporting, lysosomal 21kDa, V0 subunit c"	CAI16801
ATP synthase F0 subunit 6	AAU02441
Selenoprotein K	Q9Y6D0



Supplemental Figure 2. Co-immunoprecipitation of Tmem147 with M₁ muscarinic or V₂ vasopressin receptors in co-transfected COS-7 cells. Co-immunoprecipitation studies were carried out as described in the legend to Fig. 4 and under Materials and Methods. Lysates were prepared from COS-7 cells that had been co-transfected with Tmem147-FLAG and HA-tagged versions of the M₁ muscarinic or the V₂ vasopressin receptors. Immunoprecipitates were analyzed via Western blotting using an anti-FLAG (upper panel) or an anti-HA antibody (lower panel), respectively. COS-7 cells were co-transfected with either Tmem147-FLAG and the M₁ receptor construct (lane 1), Tmem147-FLAG and the V₂ receptor construct (lane 2), or Tmem147-FLAG and vector DNA (lane 3). Note that the anti-HA antibody detected multiple immunoreactive receptor bands ranging in size from ~60-80 kDa, most likely to heterogeneous glycosylation of the receptors.